ISSN: 1231-4005
e-ISSN: 23540133
DOI: 10.5604/01.3001.0010.3089

SELECTED MEASUREMENT AND CONTROL TECHNIQUES: EXPERIMENTAL VERIFICATION ON A LAB-SCALED OVERHEAD CRANE

Janusz Szpytko, Paweł Hyla, Agnieszka Kosoń Schab, Jarosław Smoczek

AGH University of Science and Technology
Faculty of Mechanical Engineering and Robotics
Mickiewicza Av. 30, 30-059 Krakow, Poland
tel.: +48 12 6173104
e-mail: szpytko@agh.edu.pl, hyla@agh.edu.pl
koson@agh.edu.pl, smoczek@agh.edu.pl

Abstract

This article presents three independent concepts of use high-level technique with it adaptation and implementation concerning overhead travelling crane device type. The main objective of this statement applies a solution for device workspace mapping, payload anti-sway control techniques strategy use and possibility of reliable steel construction health monitoring. In the first chapter, the vision system technology for obstacle in workspace visualization was presented. The main idea depends on use stereovision system with sets of camera mounted under the crane's trolley which movement with the crane shifts. The stereo pictures, after digital processing, were used for develop so-called dense disparity map. The described architecture allows achieving information about device surroundings and obstacle position in the workspace. As the final result was presented three-dimensional map of the device workspace with obtained result accuracy discussion. The second type of described problem developed in chapter two concern the crane control methodology of designing the anti-sway system for payload stabilizing during the crane movement. The oscillation of a payload adversely affects the accuracy of performed transportation tasks and may present a safety hazard to employees, transferred payload and surrounding objects. The invented and described method mainly base on so-called soft computing methods. The next part of the article-focused attention of problem concerning health monitoring cranes construction as other equipment's as well. The problem concerns usually the large industrial cranes carry out transportation operations in the presence of a large impact load and mechanical stresses acting overall crane's structure. The safety and efficiency of crane operations can be improved through providing the continuous structural health monitoring as well in on-line and off-line mode. The main idea allows using Metal Magnetic Memory technique for supervising and estimating steel construction actual condition. All tests and considerations were conducted on the scaled physical model of overhead travelling crane with hosting capability 150 kg.

Keywords: *overhead crane, modelling, vision systems, anti-sway control, Metal Magnetic Memory*

1. Introduction

Different types of cranes, such as bridge, gantry, jib, stacker and mobile cranes are extensively used in many industries to handle the various masses and dimensions. Contemporary it is observed inclination for standardization in the field of cranes with respect not only to the terminology but safety, ergonomic, general design principles, maintenance and operations. This propensity is expressed by the European Standards of crane design [20-22]. Crane design, control and measurement equipment are the subject of many works that have been conducted to obtain more effective, efficient and cheapest solutions satisfying these standards.

More and more sophisticated methods are proposed for designing cranes towards the reduction of cranes structures mass taking into account the safety margins [4-6, 17]. Since most of the cranes transfer a payload suspended on a flexible rope, the oscillation of a payload adversely affects the accuracy of performed transportation tasks and may present a safety hazard to employees, transferred payload and surrounding objects. This problem is extensively studied by numerous

researchers due to the challenging problem of controlling under actuated mechanical system. A comprehensive review of researchers effort, that they have put in crane modelling and control during the last five decades is summarized in [1, 10]. Most of these solutions are verified through numerical simulations carried out on the mathematical models of cranes. However, experimental model offer more confidence regarding the effectiveness and applicability of the developed solution and the feasibility of implementation.

The article summarizes the experimentally verified results of selected solutions and equipment developed and implemented on a laboratory scaled overhead traveling crane with the hoisting capacity of 150 kg. The review of those results is focused on the three research projects carried out on a laboratory stand that determines the organization of the rest of the article. Section two presents the vision-base techniques developed to identify the operating space of a crane. Section three presents the control methods implemented on a laboratory stand. Section four is addressed to the problem of continuous inspection of crane's structure using metal magnetic memory (MMM) method. The summary is delivered in section five.

2. Crane workspace identification using the vision system

At present there are available many technologies and method that can allow obtaining the digital three-dimensional model of existing object [11, 15]. However not each of them can be useful for the material handling system (MHD) workspace mapping purpose. One of the method that is really flexible in configuration and can be use in MHD environment is stereovision. Stereovision relies on the extraction the three-dimensional information from minimum two images (so-called stereo pair), taken independently at different angle view. By comparing information about a scene from these two points of view, 3D information can be gathered by examination the relative positions of objects by the two image panels. In traditional stereovision system, two cameras displaced horizontally are used to obtain two different views of the scene. In the next step by comparing these two independent taken images the relative depth information can be obtained in so-called form of disparities, which are inversely proportional to the differences in distance to the objects. Main disadvantage of stereovision use is high computing power requirement. Calculation techniques connected with dense disparity map determination needs a lot of computing power, which is caused by very demanding algorithms.

2.1. Stereovision system workspace mapping – overhead travelling crane adaptation

The overhead travelling crane (OTC) can be described like a large workspace robot [11]. If we interpret the crane hook as robot effector, then is possible to equip cranes mechanisms into cameras for acquire independent pair of images for poses information about workspace and potential obstacles in perfect stereovision mode. All consideration connected with stereovision system dedicated for the OTC must be based on crane architecture and their geometry with taking into consideration their dimensions and geometry too. Stereovision dedicated for OTC device must has possibility to measure each mechanism shifts. The measurement of each crane mechanisms shifts as well as bridge, trolley and the hoist mechanism. At presented article this was achieved by rotary encoders, its allocation on the crane was presented in Fig. 1a. The encoder connected to the hoist mechanism allows controlling rope length and thus controlling payload position in vertical dimension [7]. The technical specification of used rotary encoders was showed in the Tab. 1.

2.2. The reconstruction of crane workspace – the approach

The architecture of stereo vision system dedicated for crane was built on the cameras set suspended under crane's trolley (Fig. 1b). Two snapshots (stereo pair) were acquired as the sequence of images during the common crane/trolley movement, wherein the current location of

the crane trolley with camera holder was identified through described above incremental encoders measure system. In the Fig. 2a were presented the example of the taken stereo pair and their rectification equivalent to epipolar geometry [16].

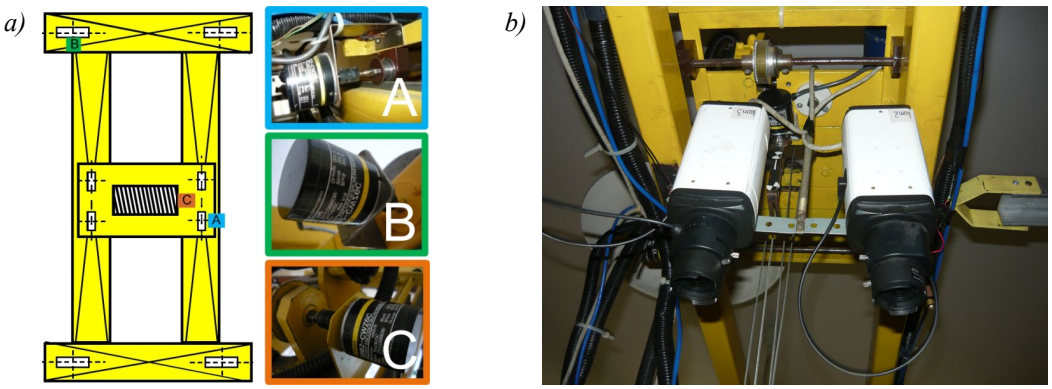

Fig. 1. From the left: a) rotary encoders placed on the physical laboratory model of the overhead travelling crane, b) stereovision camera head mounted under the crane troley

Tab. 1. Rotary encoders mounted on the overhead travelling crane model

Measurand	Encoder type	Sensor resolution	Measurement precision
Bridge position (encoder B)	Rotary encoder A/B phase	400 [imp./rot.]	7.85×10^{-4} [m]
Bridge movement velocity			7.85×10^{-4} [m/s]
Trolley position (encoder A)	Rotary encoder A/B phase	200 [imp./rot.]	3.14×10^{-4} [m]
Trolley movement velocity			3.14×10^{-4} [m/s]
Payload altitude (encoder C)	Rotary encoder A/B phase	100 [imp./rot.]	4.19×10^{-4} [m]
Hoist mechanism velocity			4.19×10^{-4} [m/s]

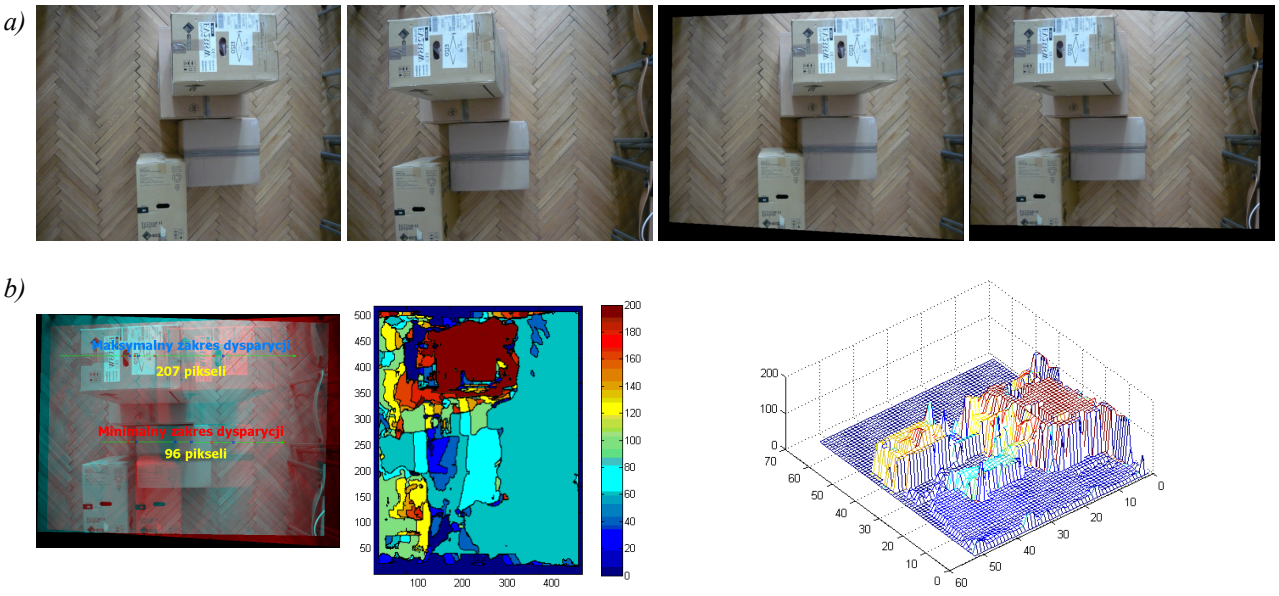

Fig. 2. a) from the left at first row: left stereo picture, right stereo picture, left and right stereo picture after epipolar transformation; b) from the left at second row: anagliph picture (left and right streo picture combined together), dense disparity map, three dimensional visualisation of the dense disparity map

The presented preprocessing is key to simplifies the problem of depth map reconstruction (Fig. 2b) from stereo pair. If the geometry of taken pictures are perfectly parallel, the disparity in one of horizontal direction does not exist [15]. Thus, dense disparity map contains only disparities allocated in one direction (Fig. 2b).

2.3. The stereovision system for overhead travelling crane workspace mapping – data validation

Verification the accuracy of the perspective representation with use stereovision system, based on the camera holder placed under the crane trolley requires developing a dedicated method. It was decided, to apply special markers with known geometry (both vertical and horizontal) to examine system performance. As markers was use several object, accurate defined with covered by uniform texture pattern. It was made six markers with the same dimension. The principal use of white-black checkered pattern was connected with eliminate errors combined with all type optical distortions possibilities. Described textures were a form of alternating black and white squares with a side length about 0.027 m.

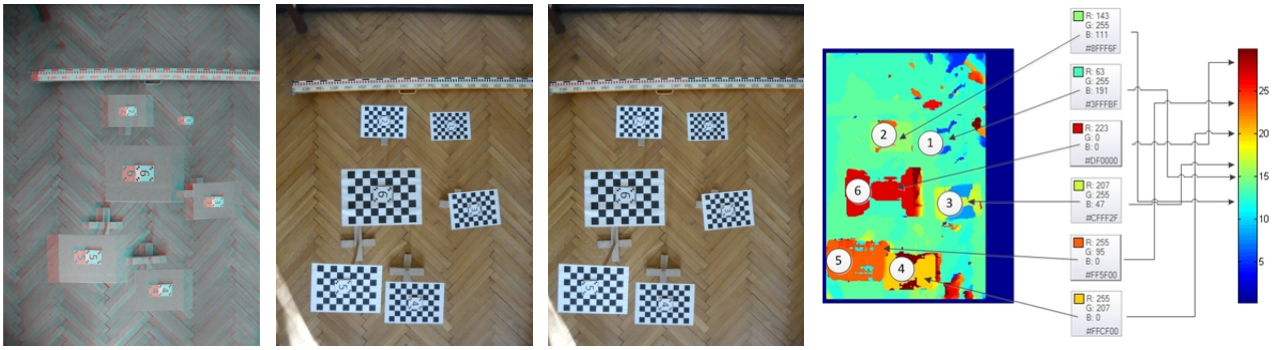

Fig. 3. From the left: anaglyph image of the accuracy stereopair control, left and right stereo picture, dense disparity map of the picture with colour extraction

Tab. 2. Estimated distance with uncertainly range calculated on the dense disparity map base

Marker number	Distance [cm]		RGB value		
	Real (measured)	Estimated distance with uncertainly range	R	G	B
6	126.7	119.8 ± 2.2	233	0	0
5	145.3	134.8 ± 2.8	255	95	0
4	171.3	161.8 ± 4.1	255	207	0
3	195.3	190.3 ± 5.6	207	255	47
2	220.9	215.7 ± 7.2	143	255	111
1	245.6	248.9 ± 9.6	63	255	191

The obtained experiment results were showed in Tab. 2. Analysing the data presented in Tab. 2 it can be seen that estimating depth for markers numbered as 1, 2 and 3, together with uncertainly valuing contains the real value. In the case of markers numbered as 4, 5 and 6 the calculate depth value are undervalued. However, the estimate error did not exceed an average 0.012 m for the minimum estimated value and 0.059 m for the maximum estimated value, which represents adequately 4.8 and 2.4 percentage points in relation to the maximum mapped height what constitute very interesting and optimistic conclusion for future research.

3. Anti-sway control strategies

The under actuated nature of crane systems causes undesirable oscillation of an unactuated payload suspended on a flexible rope manipulated by the crane's drives. The oscillation of a payload adversely affects the accuracy of performed transportation tasks and may present a safety hazard to employees, transferred payload and surrounding objects. The trade-off between

safety and efficiency of crane's operations is the challenging problem, which have been studied in numerous research works. The fast, precise and safe transfer of goods involves implementation of control techniques that effectively reduce the transient and residual oscillations in an under actuated crane system taking into consideration variation of rope length and mass of a payload.

Figure 4 presents the experimental setup used to test the anti-sway control strategies. The measurement equipment is based on the incremental encoders used for sensing the crane position and speed, rope length and payload deviation. The payload swing is measured by incremental encoder (2000 ppr) installed under the trolley and connected with fork-bottomed arm embracing the rope. The DC motor-based actuated mechanisms can be controlled by using three platforms: i) PLC (Programmable Logic Controller) FX2N48MR, ii) PAC (Programmable Automation System) with RX3i controller, iii) PC with I/O board (PCI1710HG control-measurement card) and MATLAB/RTW software.

Figure 5 presents the two control approaches developed in [12-14] and tested using the control setup presented in Fig. 1: i) generalized predictive control (GPC) with recursive least square (RLS) estimation of crane's model parameters and particle swarm optimization (PSO) algorithm employed to find the sequence of optimal control increments (Fig. 5a) [14], ii) fuzzy scheduling control (FSC) system with the payload deflection feedback estimated by a pendulum model and the fuzzy interpolator of the parameters of a pendulum model and linear controllers (Fig. 5b) [13].

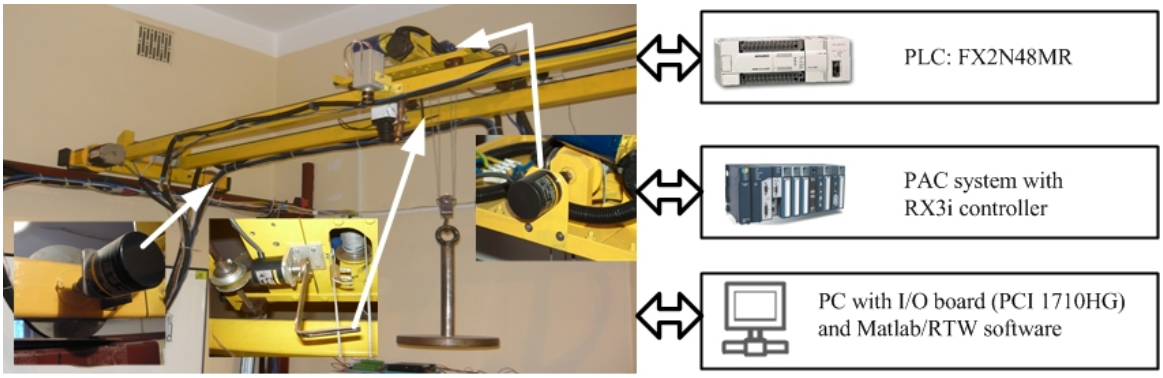

Fig. 4. Experimental setup

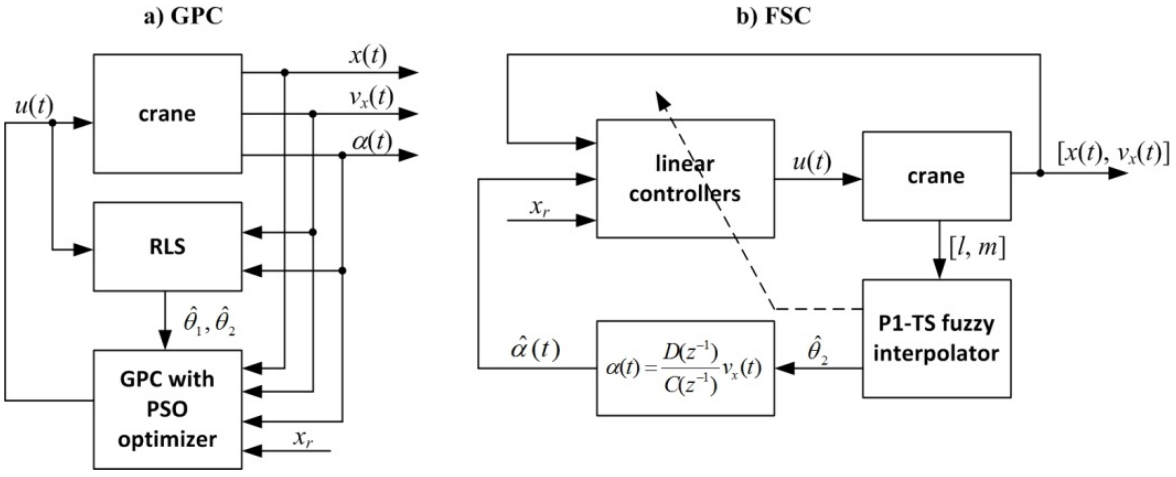

Fig. 5. Control schemes, where Θ_1 and Θ_2 are the vectors of parameters estimates

The both methods are developed based on a linear parameter varying (LPV) model of a planar crane system composed of two cascade-connected time-discrete first and second-order models showing relations between crane velocity v_x and control input signal u, and between the angle of a payload swing α and crane velocity, respectively:

$$v_x(t) = \frac{b_0}{1 + a_1 z^{-1}} u(t-1)\,, \tag{1}$$

$$\alpha(t) = \frac{d_0 + d_1 z^{-1}}{1 + c_1 z^{-1} + c_2 z^{-2}} v_x(t)\,, \tag{2}$$

where z^{-1} is the backward shift operator.

The goal of predictive control strategy is to force the crane system output to follow the reference signal x_r taking into consideration the control effort and the input and output constraints. Thus, the cost function is proposed as the sum of squared prediction errors between desired and predicted crane position, sum of weighted squares of predicted sway angle of a payload, plus weighted squares of control increments:

$$\min\ J = \sum_{j=1}^{N_p} \left(\hat{x}(t+j) - x_r(t+j)\right)^2 + \sum_{j=1}^{N_p} \lambda_{1,j} \left(\hat{\alpha}(t+j)\right)^2 + \sum_{j=1}^{N_u} \lambda_{2,j} \left(\Delta u(t+j-1)\right)^2\,, \tag{3}$$

where N_p = 30 is the prediction horizon with sample time 0.1 s, N_u = 8 control horizon, λ_1 = 3.7 and λ_2 = 0.008 are the weighting coefficients. The PSO algorithm and j-step ahead predictors are presented in [14].

The FSC is based on the feedback signals of crane position, velocity and sway angle of a payload. The fuzzy interpolator is composed of n fuzzy rules associated with the linear controllers developed using a pole placement method for n operating points at which the identification experiments were carried out to find the LPV models (1-2). The fuzzy system is applied to interpolate the parameters of the pendulum model (2) and controller based on the rope length l and mass of a payload m, which are chosen as the scheduling variables, while the model (2) estimates the payload swing, thus, the pendulum deflection in this sensorless anti-sway control approach is not required to measure. More details regarding the synthesis of the FSC are presented in [13].

Figure 6 presents the results of experiments carried out using the GPC and FSC for l = 2.2 m and m = 10 kg. The experiment with GPC was carried out for the payload deflection constraint +/– 0.06 m (estimated as the product of the rope length and sway angle $l\alpha$). The objective of the control was positioning the crane to x_r = 1 m and reducing the payload deflection within the tolerance ± 0.02 m. The GPC and FSC are compared with the Zero Vibration Derivative (ZVD) input-shaping controller. The input shaping technique was chosen for comparison as this method has been successfully implemented in the crane control applications, as it is reported in the literature [14, 18].

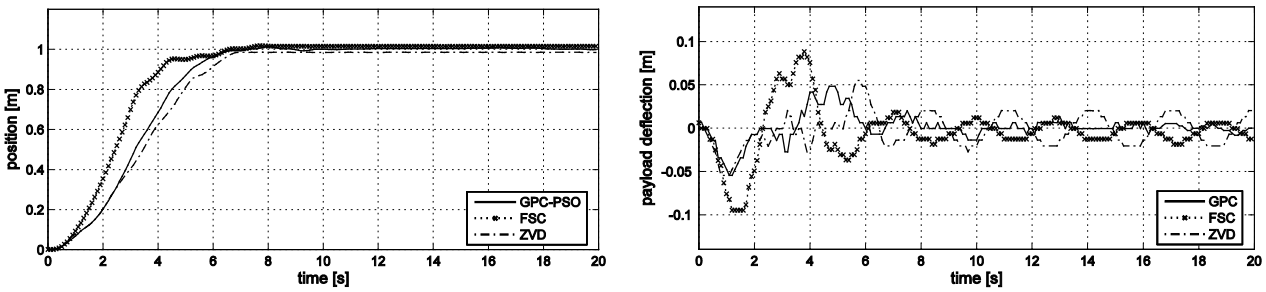

Fig. 6. Crane position and payload deviation - step responses of GPC, FSC and ZVD control schemes

The best settling time (6.2 s) is achieved using the FSC, but it is at the cost of large payload deflection in the transient state 0.095 m. The GPC and input shaper ensures better suppression of payload deflection in transient state (the amplitude of oscillation is less than 0.06 m). However, the GPC shows better settling time about 6.3 s, while the input shaper results in 6.8 s. The residual

oscillation of a payload is better damped by GPC and FSC (0.015 m) than in case of the ZVD controller (0.02 m).

The both strategies proved their effectiveness and applicability through experimental verification on a laboratory stand. They can be implemented with or without a sensor used to measure the payload swing. The experiments confirmed robustness of these control schemes against parameters variation.

4. Crane structure inspection using metal magnetic memory method

This section addresses the problem of inspection of crane's structure using MMM method. The MMM method uses natural magnetization and after-effect displayed as the magnetic memory of metal to actual strains and structural changes in products and equipment metal [2, 3, 19]. Measuring magnetic field distribution can show locations of the stress concentration zones (SCZs) and defects of material structure. The magnetization changes occurs in the zones of dislocations stable slip bands under the influence of operational or residual stresses or in the zones of maximum inhomogeneity of metal structure in new products [2]. The gradient of the H_P magnetic field tangential and normal component in SCZs is determined as follows (4)

$$K_{in} = \frac{|\Delta H_P|}{\Delta x}, \tag{4}$$

where K_{in} is the magnetic leakage field gradient or the stress intensity magnetic factor, $|\Delta H_P|$ is the absolute value of the H_P field increment related to the increment of sensor position Δx.

The gradient of SMLF correlates with the density of dislocations. Distribution of the SMLF measured by special devices can highlight areas of potential crack initiations. According to many experiments reported in the literature, the specific characteristics of varying magnetic field intensity are observed at the possible defect location. This specific change of the SMLF signal consists in changing over the sign of the normal component of SMLF, while the tangential component of SMFL reaches a local extreme. These observations are illustrated in Fig. 7 presenting the results of experiment carried out on the laboratory scaled overhead crane.

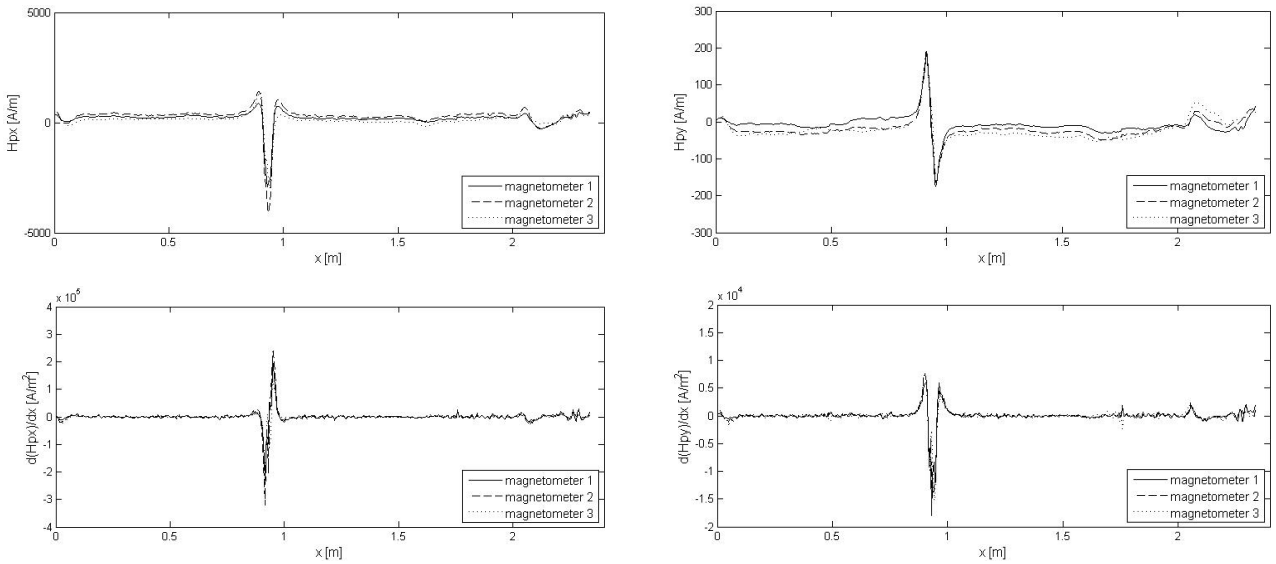

Fig. 7. Distribution of H_{Px} and H_{Py} and their gradients dH_{Px}/dx and dH_{Py}/dx along the surface of inspected crane's girder (x – axis direction)

The MMM method was employed to off-line inspection of the crane's girder: the motion mechanisms were switched off and the girder was loaded only by the mass of the trolley located at

the end of the girder. The three magnetometers were used to measure the tangential H_{Px} and normal H_{Py} components of the SMLF signal along the girder length L = 2.4 m. Fig. 7 presents the H_{Px} and H_{Py} and their gradients dH_{Px}/dx and dH_{Py}/dx. The inspection exhibited, that the potential defect is located between x = 0.93 m and x = 0.94 m from the girder origin (where x = 0 is the starting point of measurement). At this point, the H_{Px} riches the extreme value (above –4000 A/m), and the H_{Py} changes its polarity. Further analysis of the results presented in Fig. 7 are provided in next section, and compared to the SMFL signal measured under the operational variations: varying load and transient states of the trolley and hoist driving systems. However, it should be also mentioned, that the MMM technique is efficient to identify location of a possible defect, but the influence of the defect characteristics on the magnetic field intensity is not clear.

The traditional non-destructive techniques are preferable to off-line inspection due to the presence of operational variations in on-line measurements that can cause false indications of damage. The on-line inspection requires removing the effect of operational loads. The load variation, position of motion mechanisms and the transient states of driving system can influence on the effectiveness of crane's components inspection. Thus, the influence of operational variations on the SMFL signal generated by the MMM sensor is experimentally verified and quantitatively analysed in [8, 9] where the MMM technique has been applied for the inspection of a crane's girder for the different operational conditions: varying load and trolley position.

5. The summary

In the article were presented three different approach from different area of technical science with the common denominator constitute one of the MHD device type: the overhead travelling crane. However, all described research were conducted on the scaled physical model of the overhead travelling crane with double girder construction with hoist capacity of 150 kg.

In the second chapter of this article, the stereovision system for mapping crane workspace was presented with a results validation discussion delivery. The stereovision technique in described architecture allow to poses information about device surroundings during the normal device work, which constitute the main method advantage. In the third part of article, a different area approach can be visible. The crane was defined as under actuated system and the problem of payload oscillation was shown. In relation to this problem, the anti-sway control possible strategies were presented. The described solution can be implemented with or without a sensor used to measure the payload swing. The experiments confirmed robustness of these control schemes against variation parameters especially payload swings. In the fourth section authors attention consideration crane structure inspection and it health-estimating possibility. The main proposed idea was connected with use Metal Magnetic Memory effect. The proposed method uses natural magnetization phenomena as the magnetic memory of steel (in this case crane's construction) to actual strains and structural changes found. Measuring magnetic field distribution through the crane's life cycle allows discover the stress concentration zones and possible location of defects. In the article, the described technique has been applied for the inspection of a crane's girder for the different operational conditions: varying load and the trolley position.

Acknowledgement

The work has been financially supported by the Polish Ministry of Science and Higher Education.

References

[1] Abdel-Rahman, E. M., Nayfeh, A. H., Masoud, Z. N., *Dynamics and control of cranes: A review*, Journal of Vibration and Control, Vol. 9 (7), pp. 863-908, 2003.

[2] Dubov, A. A., *Methodical guideline for inspection of electric locomotive power units (frog, shaft and spline joints) using the metal magnetic memory*, Diagnostyka, Vol. 33, pp. 355-372, 2005.
[3] Dubov, A. A., *Principal features of metal magnetic memory method and inspection tools as compared to known magnetic NDT methods*, Montreal World Conference on Non Destructive Testing, August 2004.
[4] Gaska, D., Margielewicz, J., Haniszewski, T., Matyja, T., Konieczny, L., Chrost, P., *Numerical identification of the overhead traveling crane's dynamic factor caused by lifting the load off the ground*, Journal of Measurements in Engineering, Vol. 3 (1), pp. 34-35, 2015.
[5] Gaska, D., Pypno, C., *Strength and elastic stability of cranes in aspect of new and old design standards*, Mechanika 3, pp. 226-231, 2011.
[6] Haniszewski, T., *Modeling the dynamics of cargo lifting process by overhead crane for dynamic overload factor estimation*, Journal of Vibroengineering, Vol. 19 (1), pp. 75-86, 2017.
[7] Hyla, P., *Single camera-based crane sway angle measurement method,* Proceedings of the 19th International Conference of *Methods and Models in Automation and Robotics MMAR 2014,* pp. 736-741, Międzyzdroje, September 2-5, Poland, 2014.
[8] Kosoń-Schab, A., Smoczek, J., Szpytko, J., *Crane frame inspection using metal magnetic memory method*, Journal of KONES Powertrain and Transport, Vol. 23, No. 2, pp. 185-191, Warsaw 2016.
[9] Kosoń-Schab, A., Smoczek, J., Szpytko, J., *Influence of load variation on magnetic memory method-based inspection of a beam*, Hutnik – Wiadomości Hutnicze, Vol. 83 (12), pp. 532-535, 2016.
[10] Ramli, L., Mohamed, Z., Abdullahi, A. M., Jaafar, H. I., Lazim, I. M., *Control strategies for crane systems: A comprehensive review*, Mechanical Systems and Signal Processing, Vol. 95, pp. 1-23, 2017.
[11] Sawodnya, O., Aschemannb H., Lahresc S., *An automated gantry crane as a large workspace robot*, Control Engineering Practice, Vol. 10, pp. 1323-1338, 2002.
[12] Singhose, W., *Command shaping for flexible systems: A review of the first 50 years*, International Journal of Precision Engineering and Manufacturing, Vol. 10 (4), pp. 153-168, 2009.
[13] Smoczek, J., *Fuzzy crane control with sensorless payload deflection feedback for vibration reduction*, Mechanical System and Signal Processing, Vol. 46 (1), pp. 70-81, 2014.
[14] Smoczek, J., Szpytko J., *Particle swarm optimization-based multivariable generalized predictive control for an overhead crane*, IEEE/ASME Transactions on Mechatronics, Vol. 22 (1), pp. 258-268, 2017.
[15] Smoczek, J., Szpytko, J., Hyla, P., *Non-collision path planning of a payload in crane operating space*, Solid State Phenomena, Mechatronic Systems and Materials IV, Vol. 198, pp. 559-564, 2013.
[16] Szpytko, J., Hyla, P., *Disparity compute methods in three-dimensional scene reconstruction for overhead travelling crane work space visualization*, Journal of KONES Powertrain and Transport, Vol. 19, No 3, pp. 421-428, Warsaw 2012.
[17] Trąbka, A., *The impact of the support system's kinematic structure on selected kinematic and dynamic quantities of an experimental crane*, Acta Mechanica et Automatica, Vol. 8 (4), pp. 189-193, 2014.
[18] Vaughan J., Yano A., Singhose W., *Comparison of robust input shapers*, *Journal of Sound and Vibration* 315 (4-5), pp. 797-815, 2008.
[19] Zhang, Y. L., Zhou, D., Jiang, P. S., Zhang, H. C., *The state-of-the-art surveys for application of metal magnetic memory testing in remanufacturing*, Advanced Materials Research, Vol. 301-303, pp. 366-372, 2011.

[20] EN 13001−1: 2009, *Cranes. General Design. Part 1: General Principles and Requirements*.
[21] EN 13001−2:2009, *Cranes. General Design. Part 2: Load Actions*.
[22] EN 13001−3.1:2009, *Cranes. General Design. Part 3-1: Limit States and Proof of Competence of Steel Structure*.